NMR-Based Metabolomics Reveals Urinary Metabolome Modifications in Female Sprague-Dawley Rats by Cranberry Procyanidins

Haiyan Liu[a], Fariba Tayyari[b#], Arthur S. Edison[b#], Zhihua Su[c], Liwei Gu[a,*]

[a]Food Science and Human Nutrition Department, Institute of Food and Agricultural Sciences, University of Florida, Gainesville, FL 32611, United States

[b] Department of Biochemistry & Molecular Biology, Southeast Center for Integrated Metabolomics, University of Florida, Gainesville, FL 32610, United States

[c]Department of Statistics, University of Florida, Gainesville, FL 32611, United States

[#]Current address:Complex Carbohydrate Research Center, University of Georgia, Athens, Georgia 30602, United States

* Corresponding author:

Phone: (352)294-3730;Fax: (352)392-9467; Email: Lgu@ufl.edu

ABBREVIATIONS USED:

DSS, 2, 2-dimethyl-2-silapentane-5-sulfonate
HPHPA, 3-(3'-hydroxyphenyl)-3-hydroxypropanoic acid
HSQC, heteronuclear single quantum coherence
NOESY, nuclear overhauser effect spectroscopy
OPLS-DA, orthogonal projection on latent structure-discriminant analysis
PCA, principal component analysis
PHPAA, *p*-hydroxyphenylacetic acid
PLS-DA, projection on latent structure-discriminant analysis
PPAP, partially purified apple procyanidins
PPCP, partially purified cranberry procyanidins

Abstract

A ^{1}H NMR global metabolomics approach was used to investigate theurinary metabolome changes in female rats gavaged with partially purified cranberry procyanidins (PPCP) or partially purified apple procyanidins (PPAP). After collecting 24-hour baseline urine, 24 female Sprague-Dawley rats were randomly separated into two groups and gavaged with PPCP or PPAP twice using a 250 mg extracts/kg body weight dose. The 24-hour urine samples were collected after thegavage. Urine samples were analyzed using ^{1}H NMR. Multivariate analyses showed that the urinary metabolome in rats were modified after administering PPCP or PPAP compared to baseline urine metabolic profiles. 2D ^{1}H-^{13}CHSQC NMR was conducted to assist identification of discriminant metabolites. An increase of hippurate, lactate, succinate, and a decrease ofcitrate and α-ketoglutaratewere observed in rat urine after administering PPCP. Urinary levels of D-glucose, D-maltose, 3-(3'-hydroxyphenyl)-3-hydroxypropanoic acid, *p*-hydroxyphenylacetic acid, formate and phenol increased but citrate, α-ketoglutarate and creatinine decreased in rats after administering PPAP. Furthermore, the NMR analysisshowed that the metabolome in the urine of rats administered with PPCP differed from those gavaged with PPAP. Compared to PPAP, PPCP caused an increase ofurinary excretionofhippuratebut a decrease of3-(3'-hydroxyphenyl)-3-hydroxypropanoic acid, *p*-hydroxyphenylacetic acid, and phenol. These metabolome changes caused by cranberry procyanidins may help to explain its reported health benefits and identify biomarkers of cranberry procyanidin intake.

Keywords: Cranberries, procyanidins; NMR; metabolomics, multivariate analyses

1. Introduction

Cranberries (*Vaccinium macrocarpon*) are known to have various health benefits including mitigating urinary tract infection[1],delaying aging[2],decreasing the risk of cardiovascular diseases[3],and inhibiting the glycation of human hemoglobin and serum albumin[4].Many of these health-promoting properties were attributed to their procyanidin content. Procyanidinsare oligomers and polymers of(−)-epicatechin or (+)-catechinwithvarious degrees of polymerization[5].Procyanidins are classified as A-type or B-type according to their interflavan bonds. B-type procyanidins arelinked through C4 →C8 and/or C4→ C6and are widely distributed in foods[6].A-type procyanidins contain an additional ether bond between C2→O →C7 and are less common in nature. Apples contain exclusively B-type procyanidins whereasover 65% procyanidins in cranberries are A-type[7].A-type procyanidin oligomers in cranberries were reported to prevent or mitigate urinary tract infections whereas B-type ones lacked this activity. Such bioactivity was observed in cranberry juices but not in apple juices[1].

Untargeted metabolic profiling employs high-throughput analytical platforms to investigate the metabolic changes in a global manner[8].Physiological alterations due to genetic modification, pathophysiological changes, or exogenous challenges were effectively detected using a global metabolomics approach [9, 10].Diet plays a pivotal role to shape human metabolome. Part of the ingested phytochemicals from foods are absorbed through the gut barrier and metabolized. The resultant exogenous phytochemical metabolites are part of the food metabolome and may alter the endogenous metabolites [11]. Cranberry procyanidin consumption may alter the profile of endogenous metabolites. The microbial

catabolites of A-type procyanidins and altered profile of endogenous metabolites may contribute to the unique bioactivities of cranberry procyanidins. Multiple analytical platforms are used to generate the metabolite profiles of biological samples. Nuclear magnetic resonance (NMR) spectroscopy is one of the most commonly used analytical techniques. NMR spectroscopy has the advantage of being quantitative, highly reproducible, and non-selective withminimal sample preparation [8]. High-dimensional and complex data set generated from untargeted metabolomics approach can be effectively processed using multivariate statistical techniques [12]. Partial least square-discriminate analysis is a very useful statistic approach to reveal the patterns of physiological or pathological perturbation and to aid biological interpretation [13].

In the present study, we investigated the urinary metabolome modifications in female Sprague-Dawley rats after administering partially purified cranberry procyanidins (PPCP) or partially purified apple procyanidins (PPAP). We hypothesized that cranberry or apple procyanidins will modify the urinary metabolome and metabolome changes caused by cranberry procyanidins will be different from those caused by apple procyanidins. The objective of this study is to test thishypothesis using a NMR-based metabolomics approach.

2. Materials and methods

2.1. Chemicals and materials

Freeze-dried cranberry (*Vaccinium macrocarpon*) powder was provided by Ocean Spray Cranberries, Inc. (Lakeville-Middleboro, MA). Fresh granny smith apples were purchased from a local grocery store. HPLC-grade methanol, acetone, sodium phosphate dibasic anhydrous, sodium phosphate monobasic anhydrous, sodium hydroxide and

66 sodium chloride were purchased from Fischer Scientific Co. (Pittsburgh, PA).D_2O (99.9% D),
67 2, 2-dimethyl-2-silapentane-5-sulfonate (D6, 98%) was obtained from Cambridge Isotope
68 Laboratories, Inc (Tewksbury, MA). Sephadex LH-20 resin was purchased from Sigma-
69 Aldrich (St. Louis, MO). Amberlite FPX 66 resin was a product of Rohm and Haas Co.
70 (Philadelphia, PA).

71 Partially purified cranberry procyanidins were extracted from freeze dried cranberry
72 power and purified using column chromatography on Amberlite FPX 66 resins and Sephadex
73 LH-20. Briefly, one hundred and twenty grams of freeze-dried cranberry powder was
74 extracted with 1 L of methanol. Sonication was applied for 30 min on the suspension to
75 assist the extraction. Extracts obtained after vacuum filtration were combined and
76 concentrated under a partial vacuum using a rotary evaporator at 45 ^{o}C. The concentrated
77 extract was re-suspended in 20 mL of water and loaded onto a column packed with
78 Amberlite FPX 66 resins, which was eluted with 3 L of de-ionized water to remove sugars
79 and organic acids followed by 500 ml of methanol to yield cranberry sugar-free extract (5.40
80 g). The sugar-free extract (5.40 g) was suspended in 100 mL of 30% methanol and loaded
81 onto a column (5.8 × 28 cm) packed with Sephadex LH-20, which was soaked in 30%
82 methanol for over 4 hours before use. The column was eluted with 30% methanol to
83 remove anthocyanins and phenolic acids, and then eluted with 70% acetone to yield
84 partially purified cranberry procyanidins (3.95 g).Partially purified apple procyanidins (5.30 g)
85 were extracted and purified from fresh granny smith apples using a similar method. PPCP
86 contained a mixture of A- type and B- procyanidin oligomers and polymers. The total
87 procyanidin content was 51.1% (w/w) including 28.3% (w/w) of high polymers with a degree

of polymerization greater than 10. PPAP contained exclusively B-type procyanidin oligomers and polymers. The total procyanidin content was 69.1% (w/w), including 8.8% (w/w) high polymers with a degree of polymerization over 10. A detailed extraction procedure and compositional data was reported previously[14].

2.2. Animal experiments

The animal study wasapproved by the Institutional Animal Care and Use Committee at the University of Florida. Female Sprague Dawley (n=24, 220-280 g) were acclimatedfor 5 days using a purified diet free of flavonoid compounds (D10012G, Research diet Inc.,New Brunswick, NJ). After the acclimation period, rats were housed individually in a metabolic cage for 24 hours to collect 24-hour baseline urine. Afterwards, rats were randomly divided into two groups with 12 rats per group, and fasted for six hours before the metabolomics study. PPCP or PPAP were dispersed in water and administered by oral gavage at 0 and 12 hour using a dose of 250 mg extracts/kg body weight. Rats had free access to food and water after the gavage. The 24-hour urine sampleof each rat was collected starting from 0 hour after the 1stgavage. All urine samples were aliquoted and kept in a -80 ^{o}C freezer until analysis. One rat did not produce any urine sample during 24-hour urine collection period after gavaging PPAP. Therefore, this rat was excluded from this study.

2.3. 1D ^{1}H and 2D ^{1}H-^{13}C NMR

Urine samples were thawed at 4^{o}C in a cold room and then were centrifuged at 16, 000*g*for 15 min. A Gilson 215 Liquid Handler (Gilson Inc. Middleton, WI) was used to transfer 540 µl urineinto a 5-mm Bruker NMR tubehaving 60 µl of 1.5 M phosphate buffer

(pH 7.4) containing DSS (0.11 mM DSS when mixed with sample) in D_2O. The mixture in each NMR tubewas vortexed for 30 seconds. All ^{1}H-NMR spectra were collected on a 600 MHzAvance II NMR spectrometer (Bruker Biospin, Rheinstetten, Germany) equipped with a 5-mm cryoprobe, a SampleJet sample changer, and IconNMR softwarefor automation. AllNMR data were acquired at 300K. Probe tuning and matching were optimized on the first urine sample afterrandomization. A 90° pulse length, the offset of the water signal, water suppression and receiver gain for a data set were also determined on the same representative sample in each run. The probe was automatically locked to H_2O+D_2O (90%+10%) and shimmed for each sample.1D NOESY presaturated spectra for all urine samples were recorded.2D ^{1}H-^{13}C heteronuclear single quantum coherence (HSQC) were obtained ona randomly selectedrat urine after administering PPCP and a rat urine after administering PPAP to aid metabolite identification.Fourier transformed 2D ^{1}H-^{13}C HSQC files were imported to MestReNova software (Version 9.0, Mestrelab Research, Santiago de Compostela, Spain)for peak picking. ^{1}H-^{13}C HSQC peak lists were transferred to the COLMAR ^{13}C-^{1}H HSQC query web server for metabolite identification[15].

2.4. Multivariatestatistical analyses

Raw data from the spectrometerwere zero filled,Fourier transformed and phase correctedusing batch processing scripts in NMRPipe[16].Fourier transformed 1Dspectra were imported into a custom MATLAB Metabolomics Toolbox that was developed in Edison laboratoryfor referencing, removingresidual water, baseline correction, alignment, and normalization[17].We found that referencing the methyl resonance of alanine to 1.47 ppm

resulted in better database matching than referencing DSS, mostly likely because of sample pH and salt differences.Peaks were aligned using PAFFT[18].Spectra were normalized using the probabilistic quotient normalization method[19].The resultant data set was imported into SIMCA (Version 13.0.3, Umetrics, Umea, Sweden) for multivariate statistical analysis. Data were mean-centered and Pareto scaledbefore PCA, PLS-DA and OPLS-DA analyses in SIMCA. An unsupervised PCA was performed to initially examine intrinsic variation in the data set. Supervised pattern recognition methods including PLS-DA and OPLS-DA were used to extract maximum information on discriminant compounds from the data [12].Validation of the model was tested using 7-fold internal cross-validation and permutation tests 200 times. To further evaluate the predictive ability of the PLS-DA and OPLS-DA models, an external validation procedure was performed[20, 21]. The NMR metabolomics data set was split into a training set and a test set. Approximately 70% of the samples were randomly selected as training set and the remaining 30% were treated as test set. PLS-DA and OPLS-DA models were built based on the training set and obtained models were used to blindly predict the classes of the samples in the test set. This procedure was repeated 30 times and correct classification rates were calculated.

3. Results and discussion

3.1. Urinary metabolome modification after PPCP or PPAP

The score plot of PCA in **Fig. 1**showsthat rat baseline urine clustered on upper part of the graph. They were partially separatedfrom urine after administering either PPCP or PPAP. It suggested that the urinary metabolome was modified after administering procyanidins from cranberries or apples. However, no segregation of rat urine between PPCP and PPAP

was observed on PCA score plot. To further examine the metabolic changes, supervised multivariate statistic techniques were used. PLS-DA and OPLS-DA models were constructed on the urine samples in three comparisons: baseline *vs.* PPCP, baseline *vs.* PPAP, PPCP *vs.* PPAP (**Table 1**). For all three comparisons, two principal components were generated to build a PLS-DA model; one principal component and one orthogonal component were constructed to build an OPLS-DA model. R^2(cum) was calculated to evaluate the performance of the supervised models and the goodness of fit. For the baseline *vs.* PPCP comparison, the R^2Y(cum) of both PLS-DA and OPLS-DA models was 0.966(**Table 1**), indicating that about 97% of variance in Y was explained by these supervised models. The high R^2 (cum) values indicated the robustness of the supervised models[22].For the baseline *vs.* PPAP comparison, both models had a R^2Y(cum) of 0.969, suggesting that approximately 97% of variance of Y was explained by the models. Similarly, for the PPCP *vs.* PPAP comparison, supervised models with R^2Y(cum) of 0.889 was obtained **(Table 1**), suggesting that both models had an excellent goodness of fit. A complete segregation between baseline urine and urine after administering PPCP (**Fig. 2A, 2B**), between baseline urine and urine after administering PPAP (**Fig. 3A, 3B**),and between urine after administering PPCP or after PPAP (**Fig. 4A, 4B**) was observed on the score plot of PLS-DA and OPLS-DA models for all three comparisons. Furthermore, three validation methods were conducted to validate these models. When processing multivariate data with hundreds or thousands variables, one should use extreme caution for the possibility of overfitting. Accidental correlations between one or more variables may result in unreliable segregations between groups[23].To avoid overfitting, cross-validation, permutation test,and external validation

were conducted to confirm the validity and predictability of the supervised models.For baseline *vs.* PPCP comparison, Q^2(cum) obtained from cross-validation for PLS-DA and OPLS-DA was 0.853 and 0.852, respectively (**Table 1**). They were much higher than 0.5, a widely used threshold value for a good multivariate model of metabolomics data[24].Furthermore, the score plots of PLS-DA and OPLS-DA from the cross-validation also show a clear discrimination between two groups and no misclassification was observed during cross-validation (**Fig. 2C, 2D**), indicating the segregation observed on the score plot was not due to overfitting. Similarly, for the baseline *vs.* PPAP comparison, cross-validation shows a Q^2(cum) of 0.757 and 0.777 for PLS-DA and OPLS-DA models, respectively (**Table 1**).The cross-validation score plots of PLS-DA and OPLS-DA models show a clear separation between two groups and no misclassification was observed (**Fig. 3C, 3D**). As for the PPCP *vs.*PPAP comparison, the urinarymetabolic profiles of rats were modified by both PPCP and PPAP. Therefore, themagnitude of differences in urinary metabolome between PPCP and PPAP was lower than that between baseline and PPCP or baseline and PPAP group. This was demonstrated by the relatively lower Q^2(cum) of 0.656 and 0.629 obtained from PLS-DA and OPLS-DA models in the cross-validation(**Table 1**). However, these numberswere still higher than 0.5, indicating the supervised models were valid. The cross-validated score plots of PLS-DA and OPLS-DA showed a separation between two groups, although three samples had cross validation score of zero on the OPLS-DA cross-validate score plot (**Fig.4D**).

The second validation method used was the permutation test. The class labels of tested groups were permuted and randomly assigned to different observations. With the permutated class labels, 200 new supervised modelswere built, respectively. R^2 and

196 Q^2withineach model were calculated and a regression line was drawn.The Q^2-intercept
197 value obtained from the regression line should be lower than 0.05 for a valid model[25].The
198 permutation regression line was obtained from the OPLS-DA model derived from baseline
199 *vs.* PPCP comparison (**Fig.5A**)**,** baseline *vs.* PPAP comparison (**Fig. 5B**), and PPCP *vs.* PPAP
200 comparison (**Fig. 5C**). The negative Q^2 intercept suggested a good predictability of theOPLS-
201 DA models. However, the relatively high R^2 intercept indicated somewhat overfitting of the
202 supervised models. To further confirm the validity and predictability of PLS-DA and OPLS-DA
203 models, external validation was used because it is a more scrupulous and demanding
204 method[26].The results showed the correct classification rate was 95.0% and 95.6%for PLS-
205 DA and OPLS-DA model derived from baseline *vs.* PPCP comparison(**Table 1**). A correct
206 classification rate of 96.7% was obtained for both PLS-DA and OPLS-DA model derived from
207 baseline *vs.* PPAP comparison (**Table 1**). As for the PPCP *vs.* PPAP comparison, the correct
208 classification rate of 90.0% and 92.2% wasobtained from PLS-DA and OPLS-DA model,
209 respectively (**Table 1**). The external validation results demonstrated that supervised models
210 derived from rata urine NMR data had excellent predictability and were able to correctly
211 predict the unknown urine samples with a correct classification rate of above 90%. All three
212 validation tests suggested that ^{1}H NMR global metabolomics approach was effective to
213 reveal theurinary metabolome modification in female rats after administering PPCP or PPAP.

214 3.2. Discriminant metabolites identification

215 The statistical S-line^{TM} is a tailored S-plotfor NMR spectroscopy data andwas used to
216 identify the potential metabolites that contribute to the urinary metabolome modification

by PPCP or PPAP. The S-line combines the covariance (magnitude) and correlation (reliability) for the model variables and visualizes both in one graph [27].The p(ctr) is the centered loading vector of the first principal component. It was colored according to the absolute value of the correlation loading p(corr) (**Fig. 6**). A p(corr)>0.5 was selected as a significance level.The advantage of the S-line plot over the S-plot is that it displays the predictive loading in a form resembling the original NMR spectra. The discriminant metabolites were identified by comparing their NMR spectra with reported spectra[28, 29],Human Metabolome Database [30],and the COLMAR ^{13}C-^{1}H HSQC query[15].The ^{13}C-^{1}H HSQC of a urine sample and metabolites identified by COLMAR query is shown in **Fig. 7**.Discriminant metabolites were summarized in **Table 2**.

As described above, PPCP contained both A-type and B-type procyanidins, while PPAP had exclusively B-type procyanidins[14].The majority of ingested procyanidins are not absorbed in the small intestine. They reach the colon intact and are degraded by gut microbiota[6].The resultant exogenous procyanidins metabolites are part of the food metabolome and may also change the endogenous metabolome. Our previous study showed that PPCP altered the plasma metabolome in female rats and a panel of exogenous metabolites were identified for procyanidins intake [14].These plasma metabolites were derived from procyanidin degradation by gut microbiota and followed by phase II conjugation. In contrast, most urinary metabolites modified by PPCP or PPAP in the present study corresponded to endogenous metabolites except for *p*-hydroxyphenylacetic acid and 3-(3’-hydroxyphenyl)-3-hydroxypropanoic acid. Both are generated from microbial degradation of procyanidins. Previous studies showed that B-type procyanidin dimers were

239 catabolized by microbial cleavage and further degraded into hydroxyphenyl-*Y*-valerolactone,
240 which were then slowly dehydroxylated by bacteria to form phenylvaleric acids [31, 32].
241 Hydroxyphenylpropanoic acid and hydroxyphenylacetic acids were likely formed by
242 progressive shortening the aliphatic chain by α-and β-oxidation of hydroxyphenylvaleric
243 acids [32].

244 The urinary level of hippurate, succinate, lactate, unknown metabolite 1 at 7.30-7.35
245 ppm, and unknown metabolite 2 at 7.37-7.42 ppm were increased after rats were
246 administered with PPCP compared to baseline urine (**Fig. 6A**). Endogenous metabolites
247 including α-ketoglutarate and citrate were decreased after administering PPCP compared to
248 baseline samples. Similarly, rats after PPAP had a lower urinary level of α-ketoglutarate,
249 citrate and creatinine compared to baseline urine (**Fig. 6B**). PPAP caused increase ofD-
250 maltose, α-D-glucose, formate, 3-(3'-hydroxyphenyl)-3-hydroxypropanoic acid (HPHPA), *p*-
251 hydroxyphenylacetic acid (PHPAA), phenol,unknown metabolite 1 at 7.30-7.35 ppm, and
252 unknown metabolite 2 at 7.37-7.42 ppm, unknown metabolite 3 at 6.77 (s) ppm,unknown
253 metabolite 4 at 6.73 (dd) ppm, and unknown metabolite 5 at 7.04 (s) ppm (**Fig. 6B**). By
254 comparing the urinary metabolite profile of rats after PPCP and after PPAP, it was found
255 that hippurate, unknown metabolite 1 at 7.30-7.35 ppm, and unknown metabolite 2 at
256 7.37-7.42 ppmincreased after PPCP (**Fig. 6C**). Metabolites including D-maltose, 3-(3'-
257 hydroxyphenyl)-3-hydroxypropanoic acid (HPHPA), *p*-hydroxyphenylacetic acid (PHPAA),
258 phenol, unknown metabolite 3 at 6.78 (s) ppm, and unknown metabolite 4 at 6.74 (dd) ppm
259 and unknown metabolite 5 at 7.04 (s) ppm decreased after PPCP (**Fig. 6C**). The most
260 important metabolites that were responsible for the separation between baseline *vs*. PPCP

were hippurate, unknown metabolite 1 at 7.30-7.35 ppm, and unknown metabolite 2 at 7.37-7.42 ppm. The correlation loadings p(corr) of these three metabolites were 0.94, 0.91, and 0.73,which were muchhigher than the statistically significant level of 0.5. For baseline *vs*. PPAP, metabolites including 3-(3'-hydroxyphenyl)-3-hydroxypropanoic acid, *p*-hydroxyphenylacetic acid, phenol,formate, unknown metabolite 1 at 7.30-7.35 ppm, and unknown metabolite 2 at 7.37-7.42 ppm, unknown metabolite 3 at 6.78 (s) ppm, unknown metabolite 4 at 6.74 (dd) and unknown metabolite 5 at 7.04 (s) ppm had the highest correlation loadings p(corr) of 0.79, 0.84, 0.90, 0.78, 0.82, 0.73, 0.86, 0.83 and 0.92, respectively. By comparing PPCP *vs*. PPAP, the most important metabolite for the separation was an increased hippurate after PPCP with a correlation loading p(corr) of 0.94. This result was consistent with our previous finding that the urinary level of hippurate in female college students was higher after cranberry juiceconsumption[33].Another rat study also indicated that consumption of cranberry powder caused an increase in urinary excretion of hippurate. Its quantity in urine was higher than any other urinary phenolic acids[34].In addition, several exogenous metabolites including 3-(3'-hydroxyphenyl)-3-hydroxypropanoic acid, *p*-hydroxyphenylacetic acid, phenol, unknown metabolite 3 at 6.78 (s) ppm, unknown metabolite 4 at 6.74 (dd) ppmand unknown metabolite 5 at 7.04 (s) ppm also contributed to the segregation of metabolite profiles between PPCP and PPAP.

PPCP increased the urinary excretion of lactate, succinate, and hippurate. Both hippurate and succinate are the intermediates of phenylalanine metabolism, suggesting that intake of PPCP altered phenylalanine metabolism pathway at gene or protein levels. Both lactate and succinate participate in propionate metabolism, indicating an upregulation

283 of propionate metabolism by PPCP. Citrate and α-ketoglutarateare key intermediates in
284 citric acid cycle. Both compounds also participate in the metabolism of glyoxylic acid and
285 dicarboxylic acid. A reduction of citrate and α-ketoglutarate in rat urine indicated a
286 downregulation of citrate cycle and glyoxylic acid metabolism by both PPCP and PPAP.
287 Compared to baseline, PPAP increased the urinary excretion of D-glucose and D-maltose
288 that are intermediates in starch and sucrose metabolism, suggesting that PPAP had an
289 impact on the metabolism of carbohydrates in rats. Previous research suggested that
290 procyanidins prevented or alleviated type 2 diabetes in part by inhibiting enzymes in starch
291 digestion[35, 36]. Phenol, *p*-hydroxyphenylacetic acid and 3-(3'-hydroxyphenyl)-3-
292 hydroxypropanoic acid also increased after PPAP. They are microbial metabolites of
293 procyanidins by gut microbiota[6]. Phenol and *p*-hydroxyphenylacetic acid may also
294 originate from tyrosine metabolism. Phenol is a metabolite degraded directly from tyrosine.
295 *p*-hydroxyphenylacetic acid is an intermediate converted from 4-
296 hydroxyphenylacetaldehyde which is oxidized from *p*-tyramine in the pathwayof tyrosine
297 metabolism. An increase of formate after PPAP suggested an alternation of pyruvate
298 metabolism pathway.

299 In conclusion, female Sprague-Dawley rat urinary metabolome modification after
300 administering PPCP or PPAP was detected using a globalNMR-based metabolomics
301 approach. PPCP caused an increase of hippurate, lactate, succinate, but a decrease of
302 citrate and α-ketoglutarate in rat urine after administering PPCP compared to baseline urine.
303 The urinary level of α-D-glucose,D-maltose, 3-(3'-hydroxyphenyl)-3-hydroxypropanoic acid,
304 *p*-hydroxyphenylacetic acid and phenol were increased butcitrate, α-ketoglutarate and

creatinine were decreased after administering PPAP compared to baseline urine. The metabolite profilesafter administering PPCP differed from those after PPAP. Discriminating metabolites included hippurate which was higher in rat urine after PPCP. D-maltose, 3-(3'-hydroxyphenyl)-3-hydroxypropanoic acid, *p*-hydroxyphenylacetic acid and phenol were lower after PPCP. This study highlighted the importance of using an untargeted approach to reveal the metabolome modification by diet intervention.Urinary metabolome modifications discovered in this study complemented previous findings on plasma metabolome changes in female rats after cranberry procyanidins intake. In addition, the metabolic differences observed in the present study were consistent with our previous findings in human and provided additional information that may help to explain the unique bioactivity of cranberry procyanidins in mitigating urinary tract infections.

ACKNOWLEDGEMENTS

NMR metabolomics data were acquired in the Southeast Center for Integrated Metabolomics at the University of Florida (NIH/NIDDK 1U24DK097209-01A1) using the National High Magnetic Field Laboratory's AMRIS Facility, which is supported by National Science Foundation Cooperative Agreement No. DMR-1157490 and the State of Florida. Zhihua Su is supported by a grant (DMS-1407460) from National Science Foundation. The authors thank Ramadan Ajredini for his help in sample preparation

REFERENCES

[1] Howell AB, Reed JD, Krueger CG, Winterbottom R, Cunningham DG, Leahy M. A-type cranberry proanthocyanidins and uropathogenic bacterial anti-adhesion activity. Phytochemistry. 2005;66:2281-91.

[2] Wilson T, Singh AP, Vorsa N, Goettl CD, Kittleson KM, Roe CM, et al. Human glycemic response and phenolic content of unsweetened cranberry juice. Journal of Medicinal Food. 2008;11:46-54.

[3] Caton PW, Pothecary MR, Lees DM, Khan NQ, Wood EG, Shoji T, et al. Regulation of Vascular Endothelial Function by Procyanidin-Rich Foods and Beverages†. Journal of Agricultural and Food Chemistry. 2010;58:4008-13.

[4] Liu H, Liu H, Wang W, Khoo C, Taylor J, Gu L. Cranberry phytochemicals inhibit glycation of human hemoglobin and serum albumin by scavenging reactive carbonyls. Food & Function. 2011;2:475-82.

[5] Gu L, Kelm M, Hammerstone JF, Beecher G, Cunningham D, Vannozzi S, et al. Fractionation of polymeric procyanidins from lowbush blueberry and quantification of procyanidins in selected foods with an optimized normal-phase HPLC-MS fluorescent detection method. Journal of Agricultural and Food Chemistry. 2002;50:4852-60.

[6] Ou K, Gu L. Absorption and metabolism of proanthocyanidins. Journal of Functional Foods. 2014;7:43-53.

[7] Prior RL, Gu L. Occurrence and biological significance of proanthocyanidins in the American diet. Phytochemistry. 2005;66:2264-80.

[8] Dunn WB, Broadhurst DI, Atherton HJ, Goodacre R, Griffin JL. Systems level studies of mammalian metabolomes: the roles of mass spectrometry and nuclear magnetic resonance spectroscopy. Chemical Society Reviews. 2011;40:387-426.

[9] Griffin JL. The Cinderella story of metabolic profiling: does metabolomics get to go to the functional genomics ball? Philosophical Transactions of the Royal Society B: Biological Sciences. 2006;361:147-61.

[10] Nicholson JK, Lindon JC, Holmes E. 'Metabonomics': understanding the metabolic responses of living systems to pathophysiological stimuli via multivariate statistical analysis of biological NMR spectroscopic data. Xenobiotica. 1999;29:1181-9.

[11] Manach C, Hubert J, Llorach R, Scalbert A. The complex links between dietary phytochemicals and human health deciphered by metabolomics. Molecular nutrition & food research. 2009;53:1303-15.

[12] Bylesjö M, Rantalainen M, Cloarec O, Nicholson JK, Holmes E, Trygg J. OPLS discriminant analysis: combining the strengths of PLS‐DA and SIMCA classification. Journal of Chemometrics. 2006;20:341-51.

[13] Marchesi JR, Holmes E, Khan F, Kochhar S, Scanlan P, Shanahan F, et al. Rapid and noninvasive metabonomic characterization of inflammatory bowel disease. Journal of proteome research. 2007;6:546-51.

[14] Liu H, Garrett TJ, Tayyari F, Gu L. Profiling the metabolome changes caused by cranberry procyanidins in plasma of female rats using ^{1}H NMR and UHPLC‐Q‐

Orbitrap‐HRMS global metabolomics approaches. Molecular Nutrition & Food Research. 2015;59:2107-18.
[15] Bingol K, Li D-W, Bruschweiler-Li L, Cabrera OA, Megraw T, Zhang F, et al. Unified and Isomer-Specific NMR Metabolomics Database for the Accurate Analysis of 13C–1H HSQC Spectra. ACS Chemical Biology. 2014;10:452-9.
[16] Delaglio F, Grzesiek S, Vuister GW, Zhu G, Pfeifer J, Bax A. NMRPipe: a multidimensional spectral processing system based on UNIX pipes. Journal of Biomolecular NMR. 1995;6:277-93.
[17] Robinette SL, Ajredini R, Rasheed H, Zeinomar A, Schroeder FC, Dossey AT, et al. Hierarchical alignment and full resolution pattern recognition of 2D NMR Spectra: Application to nematode chemical ecology. Analytical Chemistry. 2011;83:1649-57.
[18] Vu T, Valkenborg D, Smets K, Verwaest K, Dommisse R, Lemiere F, et al. An integrated workflow for robust alignment and simplified quantitative analysis of NMR spectrometry data. BMC Bioinformatics. 2011;12:405.
[19] Dieterle F, Ross A, Schlotterbeck G, Senn H. Probabilistic Quotient Normalization as Robust Method to Account for Dilution of Complex Biological Mixtures. Application in 1H NMR Metabonomics. Analytical Chemistry. 2006;78:4281-90.
[20] Llorach R, Garrido I, Monagas M, Urpi-Sarda M, Tulipani S, Bartolome B, et al. Metabolomics study of human urinary metabolome modifications after intake of almond (Prunus dulcis (Mill.) DA Webb) skin polyphenols. Journal of Proteome Research. 2010;9:5859-67.
[21] Brindle JT, Antti H, Holmes E, Tranter G, Nicholson JK, Bethell HW, et al. Rapid and noninvasive diagnosis of the presence and severity of coronary heart disease using 1H-NMR-based metabonomics. Nature Medicine. 2002;8:1439-45.
[22] Llorach R, Urpi-Sarda M, Jauregui O, Monagas M, Andres-Lacueva C. An LC-MS-based metabolomics approach for exploring urinary metabolome modifications after cocoa consumption. Journal of Proteome Research. 2009;8:5060-8.
[23] Kemsley EK, Le Gall G, Dainty JR, Watson AD, Harvey LJ, Tapp HS, et al. Multivariate techniques and their application in nutrition: a metabolomics case study. British Journal of Nutrition. 2007;98:1-14.
[24] Hawkins DM, Basak SC, Mills D. Assessing model fit by cross-validation. Journal of Chemical Information and Computer Sciences. 2003;43:579-86.
[25] Kang J, Choi M-Y, Kang S, Kwon HN, Wen H, Lee CH, et al. Application of a 1H nuclear magnetic resonance (NMR) metabolomics approach combined with orthogonal projections to latent structure-discriminant analysis as an efficient tool for discriminating between Korean and Chinese herbal medicines. Journal of Agricultural and Food Chemistry. 2008;56:11589-95.
[26] Eriksson L, Byrne T, Johansson E, Trygg J, Vikstrom C. Multi-and megavariate data analysis: basic principles and appications. 3rd ed: Umetrics Academy; 2013.
[27] Wiklund S, Johansson E, Sjöström L, Mellerowicz EJ, Edlund U, Shockcor JP, et al. Visualization of GC/TOF-MS-based metabolomics data for identification of biochemically interesting compounds using OPLS class models. Analytical Chemistry. 2008;80:115-22.
[28] Bouatra S, Aziat F, Mandal R, Guo AC, Wilson MR, Knox C, et al. The Human Urine Metabolome. PloS One. 2013;8:e73076.

[29] Psychogios N, Hau DD, Peng J, Guo AC, Mandal R, Bouatra S, et al. The human serum metabolome. PloS One. 2011;6:e16957.
[30] Wishart DS, Tzur D, Knox C, Eisner R, Guo AC, Young N, et al. HMDB: the human metabolome database. Nucleic Acids Research. 2007;35:D521-D6.
[31] Stoupi S, Williamson G, Drynan JW, Barron D, Clifford MN. A comparison of the in vitro biotransformation of (−)-epicatechin and procyanidin B2 by human faecal microbiota. Molecular nutrition & food research. 2010;54:747-59.
[32] Sánchez-Patán F, Cueva C, Monagas M, Walton GE, Gibson GR, Martín-Álvarez PJ, et al. Gut microbial catabolism of grape seed flavan-3-ols by human faecal microbiota. Targetted analysis of precursor compounds, intermediate metabolites and end-products. Food Chemistry. 2012;131:337-47.
[33] Liu H, Tayyari F, Khoo C, Gu L. A 1 H NMR-based approach to investigate metabolomic differences in the plasma and urine of young women after cranberry juice or apple juice consumption. Journal of Functional Foods. 2015;14:76-86.
[34] Prior RL, Rogers TR, Khanal RC, Wilkes SE, Wu X, Howard LR. Urinary Excretion of Phenolic Acids in Rats Fed Cranberry. Journal of Agricultural and Food Chemistry. 2010;58:3940-9.
[35] Lee YA, Cho EJ, Tanaka T, Yokozawa T. Inhibitory activities of proanthocyanidins from persimmon against oxidative stress and digestive enzymes related to diabetes. Journal of Nutritional Science and Vitaminology. 2007;53:287-92.
[36] Gu Y, Hurst WJ, Stuart DA, Lambert JD. Inhibition of key digestive enzymes by cocoa extracts and procyanidins. Journal of Agricultural and Food Chemistry. 2011;59:5305-11.

Table 1

Summary of Parameters for PLS-DA and OPLS-DA Models for Rat Baseline Urine and Urine after Administering PPCPor PPCP by Oral Gavage

	Baseline *vs.* PPCP		Baseline *vs.* PPAP		PPCP *vs.* PPAP	
	PLS-DA	OPLS-DA	PLS-DA	OPLS-DA	PLS-DA	OPLS-DA
N[a]	2	1P[c]+1O[d]	2	1P[c]+1O[d]	2	1P[c]+1O[d]
$R^2X(cum)$[b]	0.248	0.248	0.326	0.326	0.278	0.278
$R^2Y(cum)$[b]	0.966	0.966	0.969	0.969	0.889	0.889
$Q^2(cum)$[b]	0.853	0.852	0.757	0.777	0.656	0.629
*Correct Classification Rate	0.950±0.089	0.956±0.075	0.967±0.068	0.967±0.068	0.900±0.143	0.922±0.105

[a] N: number of components.

[b] R^2X (cum)and R^2Y (cum) are the cumulative modeled variations in the X and Y matrix, respectively. Q^2Y (cum) is the cumulative predicted variation in the Y matrix.

[c] Predictive component.

[d] Orthogonal component.

*Correct classification rate was obtained from external validation procedure repeated for 30 times.

Table 2

Summary of the Metabolite Profile Changes in Rat Baseline Urine and Urine after Administering PPCP or PPCP by Oral Gavage

Discriminant Metabolites	Chemical Shift (multiplicity)	PPCP *vs*. Baseline [a]	PPAP *vs*. Baseline [b]	PPCP *vs*. PPAP [c]
Lactate*	1.32 (d)	↑	----	----
Succinate*	2.39 (s)	↑	----	----
Citrate*	2.52 (d), 2.67 (d)	↓	↓	----
α-ketoglutarate*	2.43 (t), 2.99 (t)	↓	↓	----
Creatinine*	3.03 (s), 4.04 (s)	----	↓	----
D-glucose*	5.23 (d), 4.65 (d)	----	↑	----
D-maltose*	3.26 (dd), 3.42 (t), 3.58 (m), 3.62 (m), 3.71 (m), 3.76 (m), 3.83 (m), 3.89 (m), 3.96 (m), 5.40 (d), 5.25 (d)	----	↑	↓
Phenol	6.94 (d)	----	↑	↓
p-hydroxyphenylacetic acid (PHPAA)*	7.15 (d), 6.85 (d)	----	↑	↓
3-(3'-hydroxyphenyl)-3-hydroxypropanoic acid (HPHPA)	5.05 (dd), 6.84 (dd), 6.97 (d), 7.22 (t)	----	↑	↓
Hippurate*	7.53 (t), 7.62 (t), 7.82 (d)	↑	----	↑
Formate	8.45 (s)	----	↑	----
Unknown metabolite 1	7.30-7.35	↑	↑	↑
Unknown metabolite 2	7.37-7.42	↑	↑	↑
Unknown metabolite 3	6.77 (s)	----	↑	↓
Unknown metabolite 4	6.73 (dd)	----	↑	↓
Unknown metabolite 5	7.04 (s)	----	↑	↓

[a]Arrows indicated a decrease or increase in metabolites detected in rat urine after PPCP compared to baseline.

[b]Arrows indicated a decrease or increase in metabolites detected in rat urine after PPAP compared to baseline.

[c]Arrows indicated a decrease or increase in metabolites detected in rat urine after PPCP compared to PPAP.

*Metabolite identification was confirmedby COLMAR ^{13}C-^{1}H HSQC query.[15]

Figure Captions:

Fig. 1. The PCA score plot of rat baseline urine and urine after administering PPCP and PPAP. Green squares: rat baseline urine. Red squares: rat urine after administering PPAP.Blue squares: rat urine after administering PPCP. Each square represents an individual rat.

Fig.2. The PLS-DA (A), OPLS-DA (B) score plots, PLS-DA (C) and OPLS-DA (D) cross-validated score plots of rat baseline urine and urine after administering PPCP. Green squares: rat baseline urine before administeringPPCP. Blue squares: rat urineafter administeringPPCP. Each square represents an individual rat.

Fig.3. The PLS-DA (A), OPLS-DA (B) score plots, PLS-DA (C) and OPLS-DA (D) cross-validated score plots of rat baseline urine and urine after administering PPAP. Green squares: rat baseline urine before administeringPPAP. Red squares: rat urineafter administeringPPAP. Each square represents an individual rat.

Fig.4. The PLS-DA (A), OPLS-DA (B) score plots, PLS-DA (C) and OPLS-DA (D) cross-validated score plots of rat urine after administering PPCP or PPAP. Blue squares: rat urine after administeringPPCP. Red squares: rat urineafter administeringPPAP. Each square represents an individual rat.

Fig. 5. Validation plot obtained from 200 permutation tests for the OPLS-DA models of rat baseline urine *vs.* urine after administering PPAP (A), rat baseline urine *vs.* urine after administering PPCP (B), and urine after administering PPCP *vs.*PPAP (C).

Fig.6. S-line associated with the OPLS score plots of data derived from rat baseline urine *vs*. urine after administering PPCP (A), rat baseline urine *vs*. urine after administering PPAP (B), and urine after administering PPCP *vs.* PPAP (C). The x-axis is chemical shift derived from NMR spectra. The y-axis p(ctr)[1] is the centered loading vector of the first principal component. P(ctrl)[1] is colored according to the absolute value of the correlation loading p(corr). P(corr)>0.5 is selected as significance level. Rectangle areas enclosed by dotted line are zoomed out and depicted as insets in the figure.

Fig.7. ^{13}C-^{1}H HSQC of rat urine after administering PPCP and metabolites identified after COLMAR query.

Fig. 1.

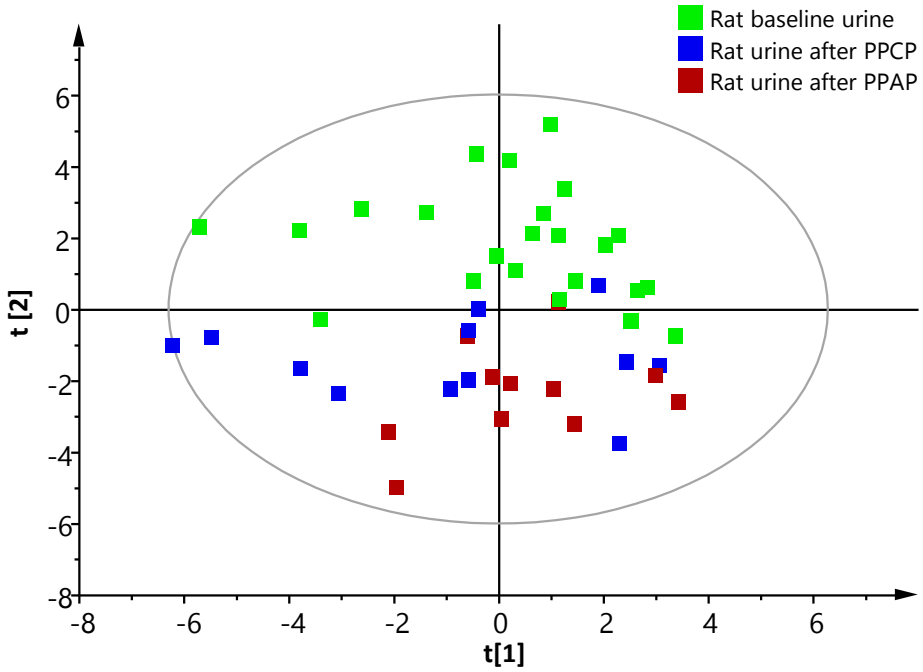
Rat baseline urine
Rat urine after PPCP
Rat urine after PPAP
t [2]
t[1]
6
4
2
0
-2
-4
-6
-8
-8
-6
-4
-2
0
2
4
6

Fig. 2

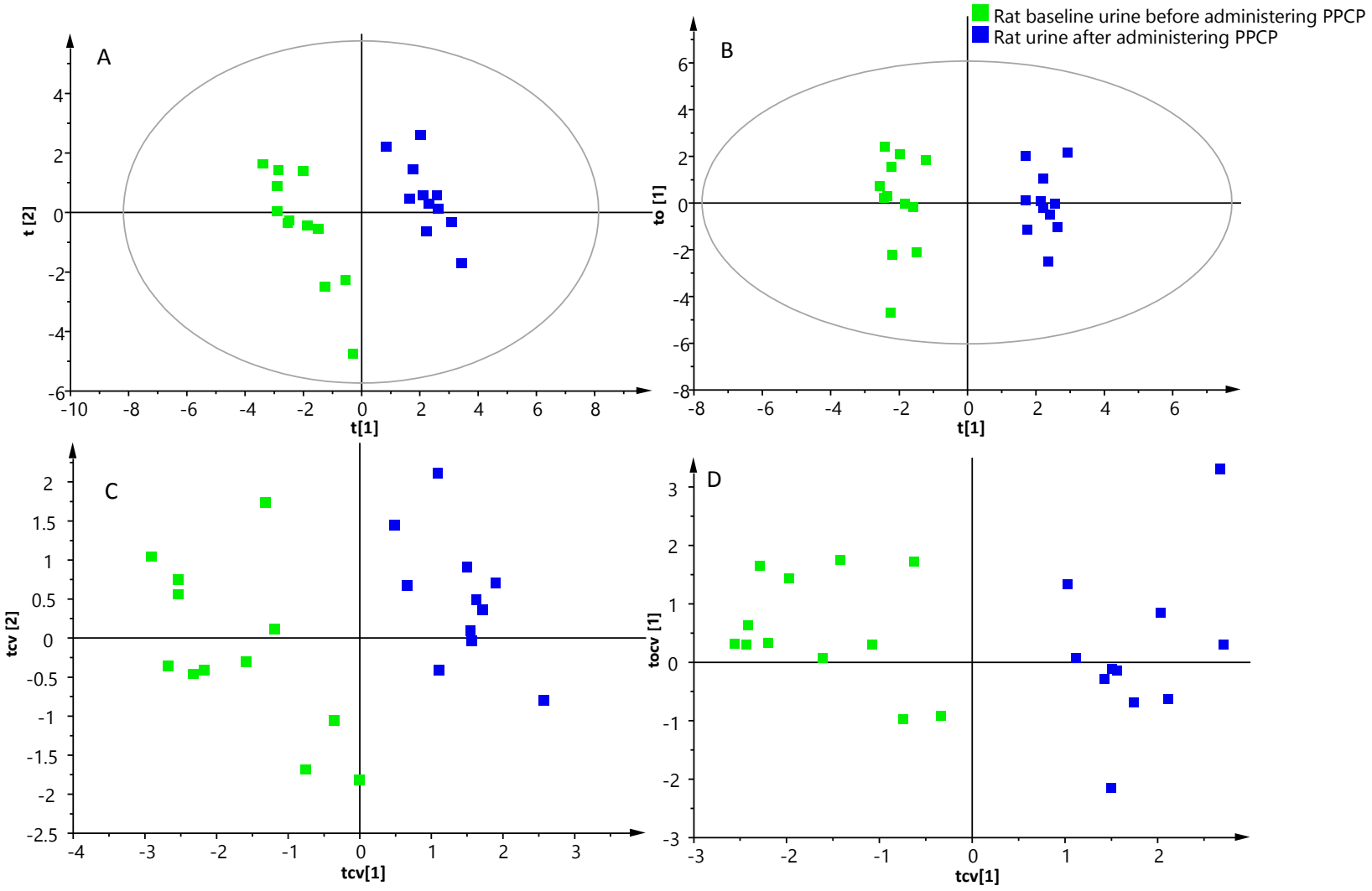
Rat baseline urine before administering PPCP
Rat urine after administering PPCP
A
B
C
D
t [2]
t[1]
to [1]
t[1]
tcv [2]
tcv[1]
tocv [1]
tcv[1]

Fig. 3.

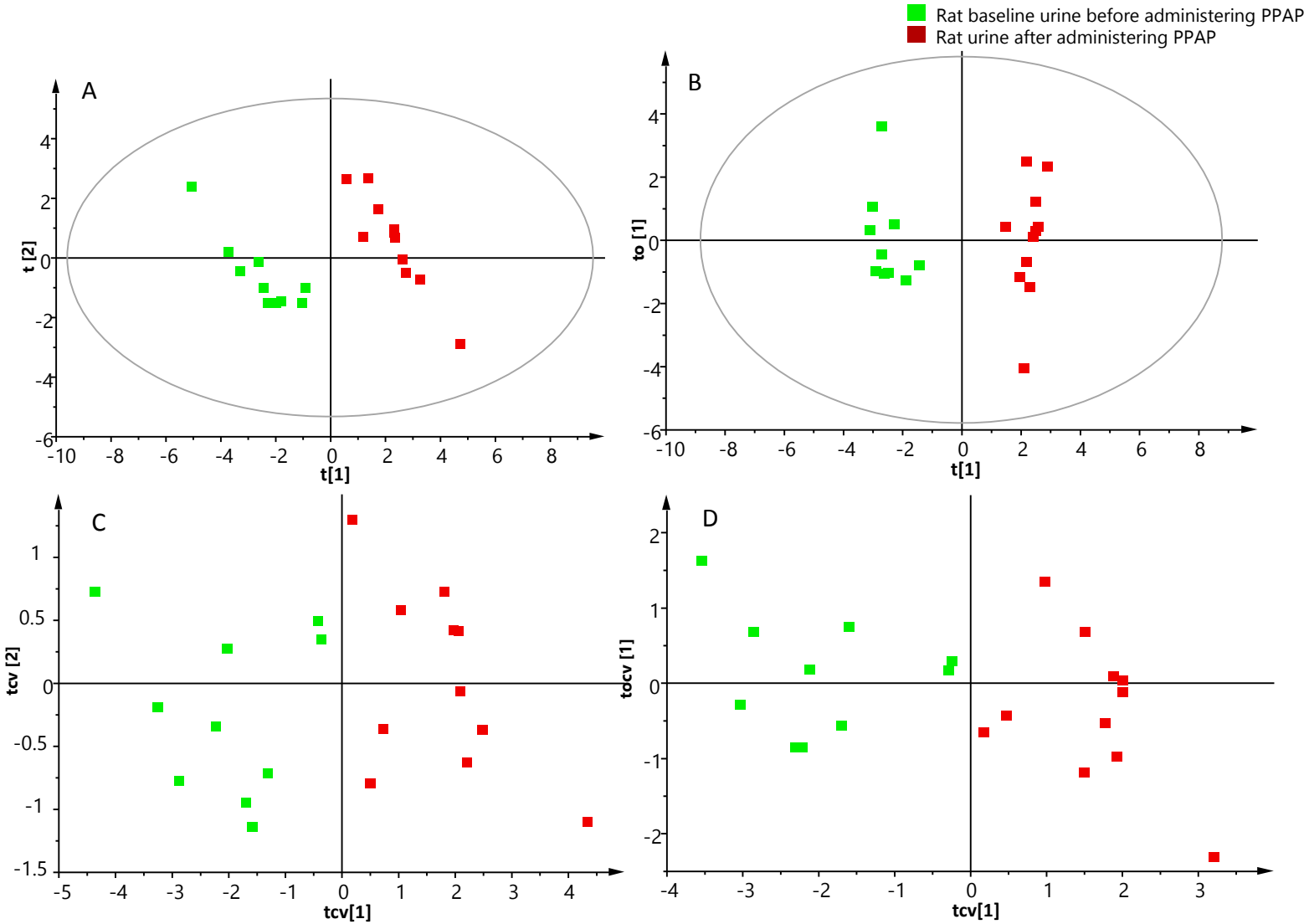
Rat baseline urine before administering PPAP
Rat urine after administering PPAP
A
t [2]
t[1]
B
to [1]
t[1]
C
tcv [2]
tcv[1]
D
tocv [1]
tcv[1]

Fig. 4.

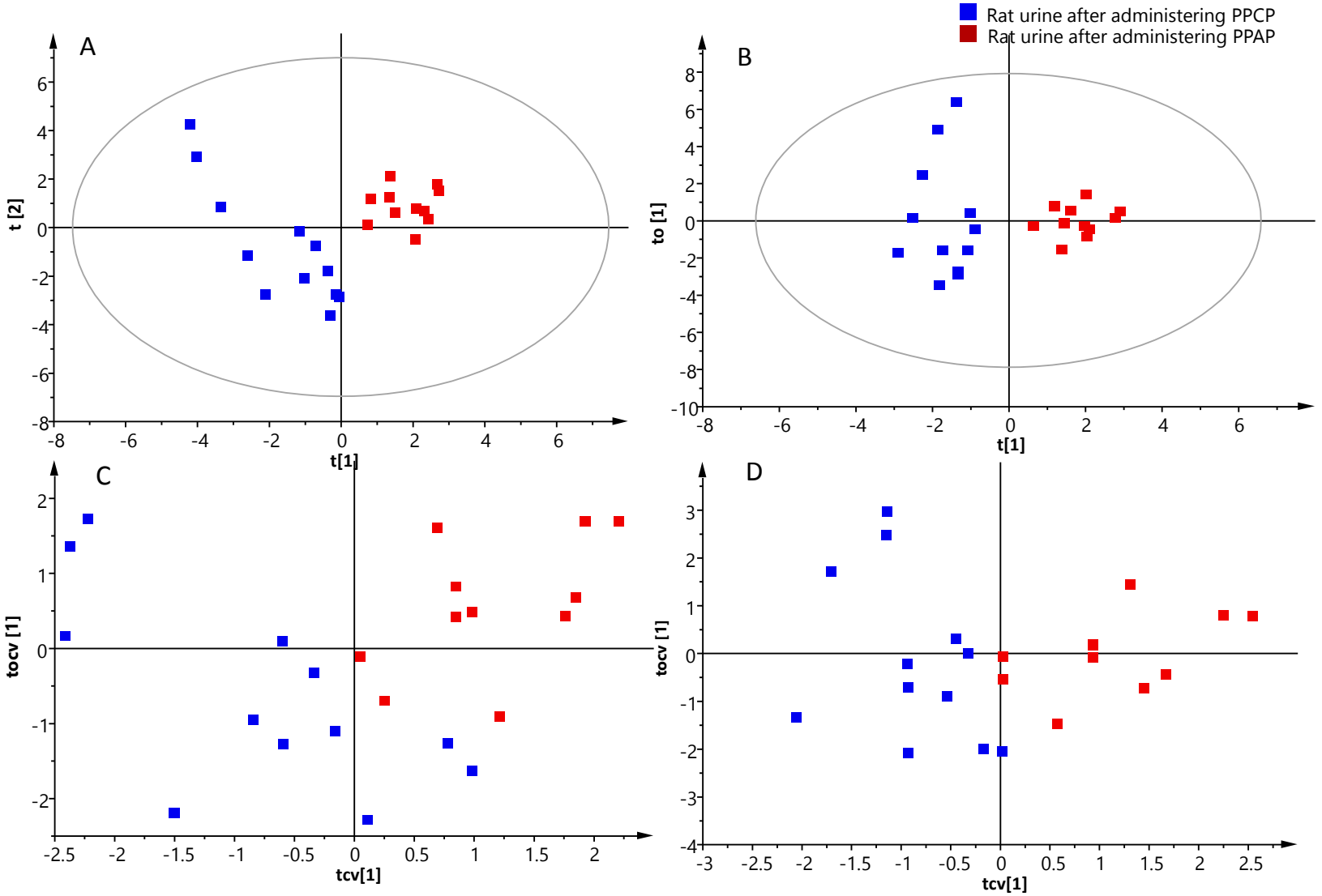
A
B
C
D
Rat urine after administering PPCP
Rat urine after administering PPAP
t [2]
t[1]
to [1]
t[1]
tocv [1]
tcv[1]
tocv [1]
tcv[1]

Fig. 5.

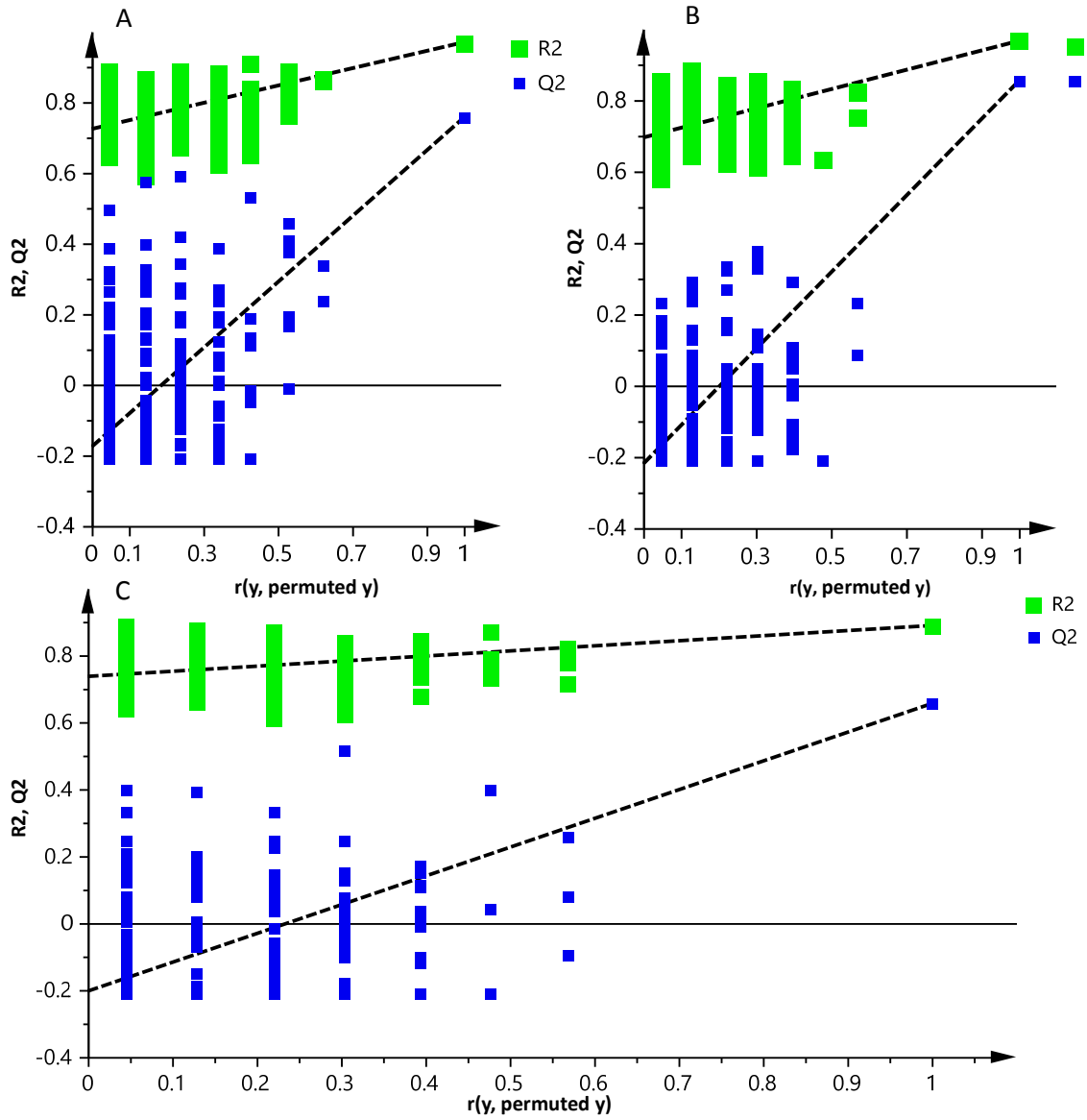

Fig. 6.

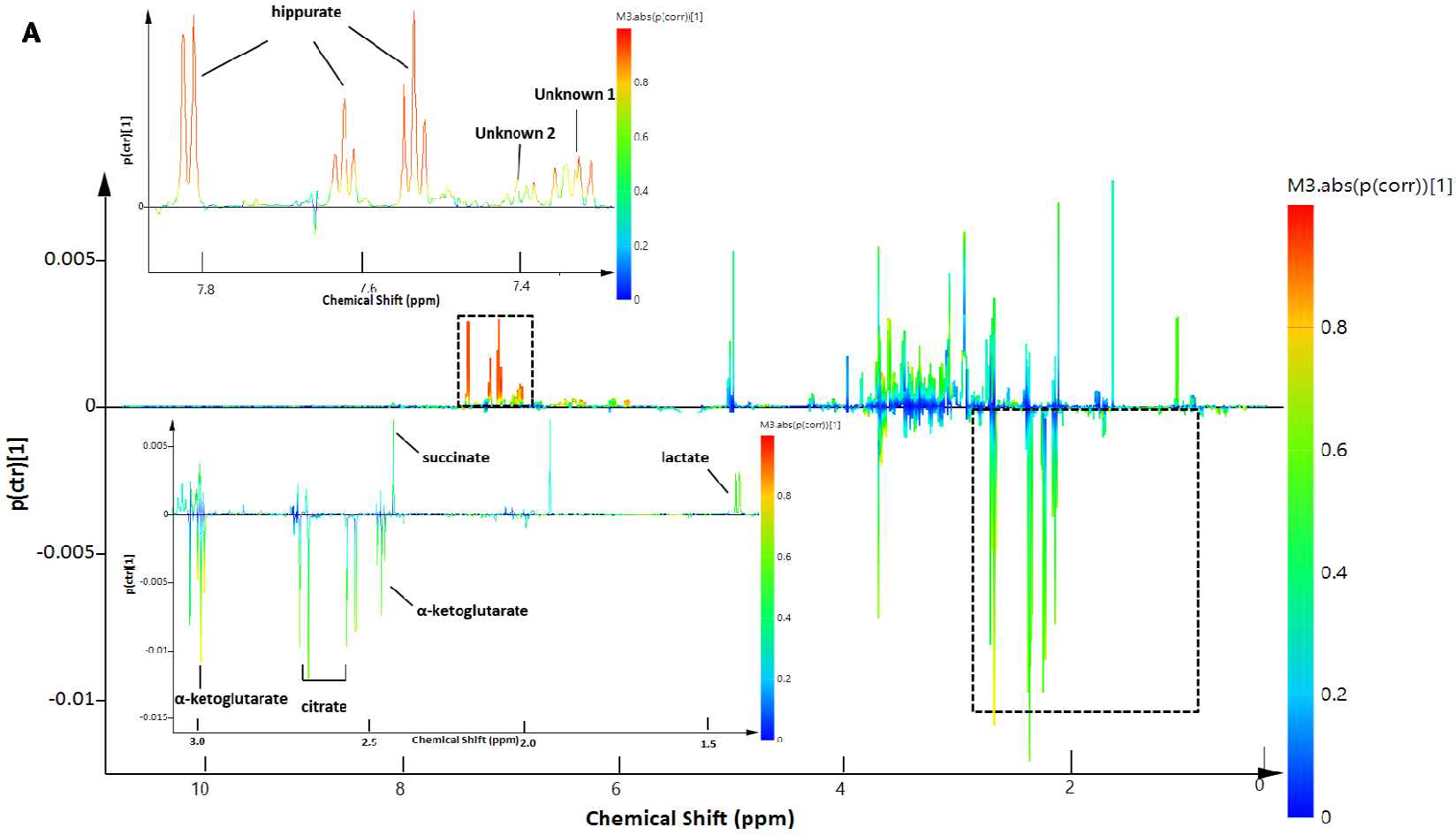
A
hippurate
Unknown 1
Unknown 2
M3.abs(p(corr))[1]
p(corr)[1]
Chemical Shift (ppm)
succinate
lactate
α-ketoglutarate
α-ketoglutarate
citrate
0.005
0
-0.005
-0.01
10
8
6
4
2
0
0.8
0.6
0.4
0.2
0

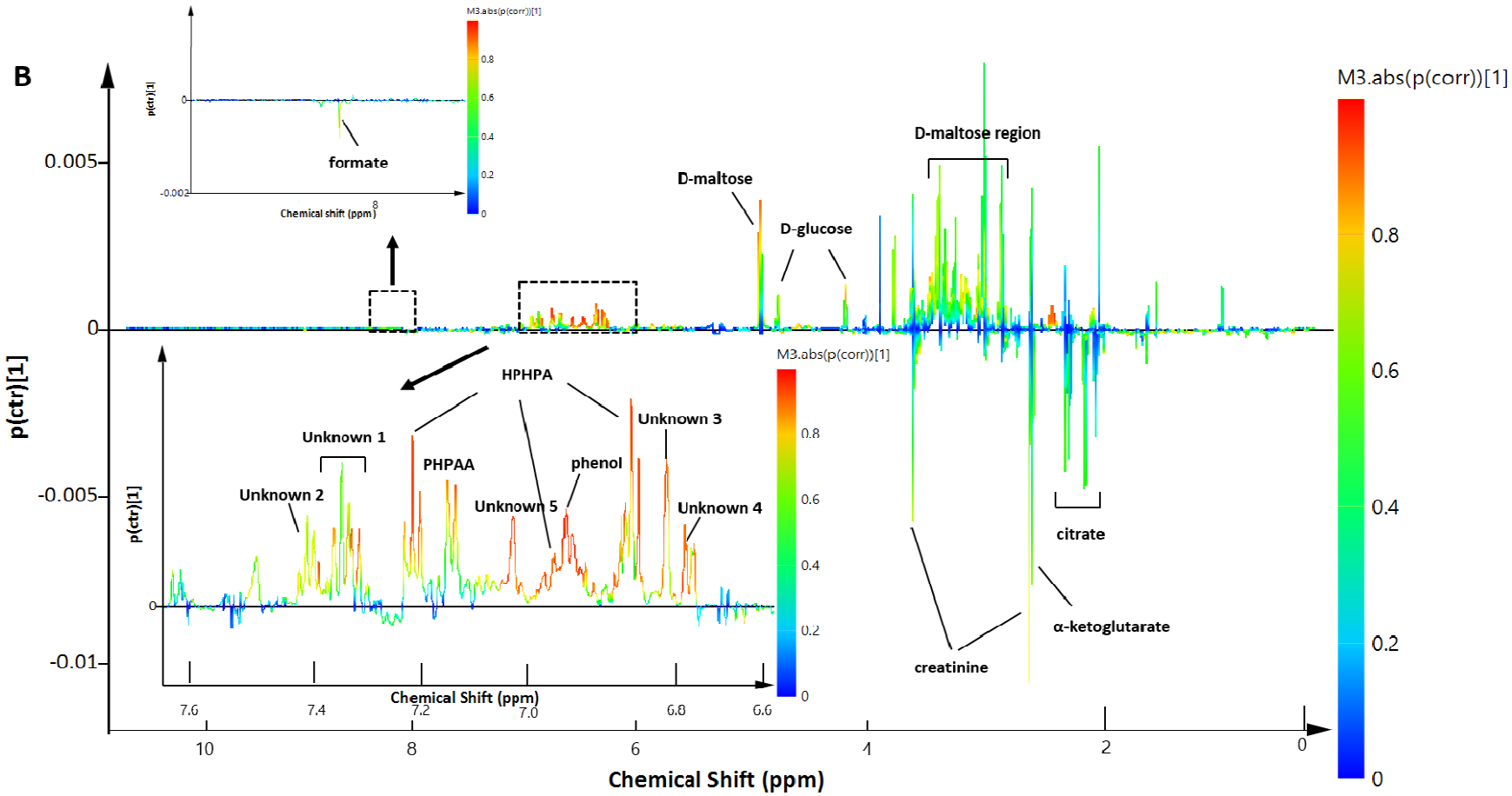
B
M3.abs(p(corr))[1]
p(ctr)[1]
0.005
0
-0.005
-0.01
formate
D-maltose
D-glucose
D-maltose region
citrate
α-ketoglutarate
creatinine
HPHPA
Unknown 1
Unknown 2
PHPAA
Unknown 5
phenol
Unknown 3
Unknown 4
Chemical Shift (ppm)
10
8
6
4
2
0
0.8
0.6
0.4
0.2
0

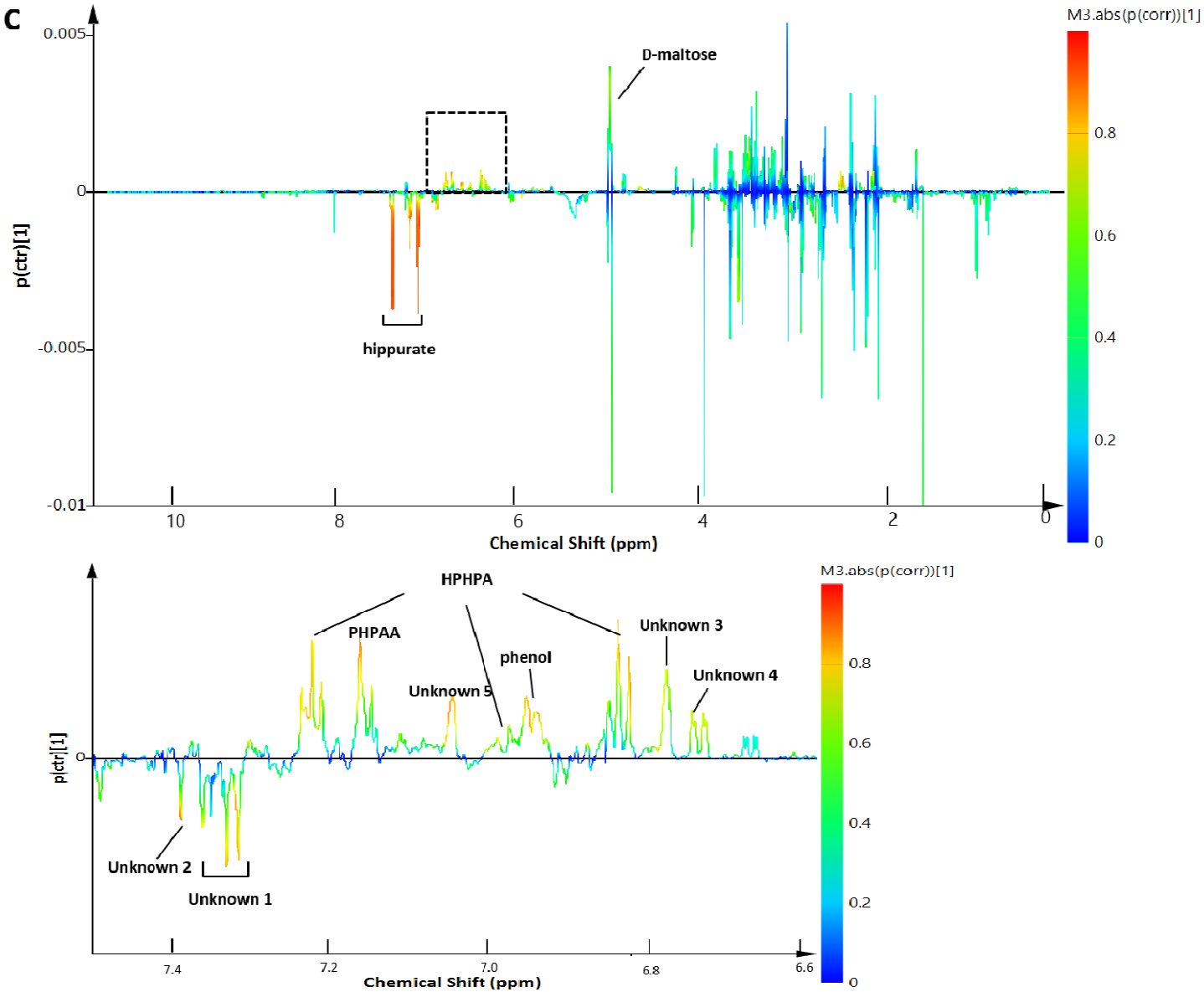
C
M3.abs(p(corr))[1]
0.005
0
-0.005
-0.01
p(ctr)[1]
D-maltose
hippurate
10
8
6
4
2
0
Chemical Shift (ppm)
0.8
0.6
0.4
0.2
0
HPHPA
PHPAA
phenol
Unknown 3
Unknown 4
Unknown 5
Unknown 2
Unknown 1
7.4
7.2
7.0
6.8
6.6

Fig. 7

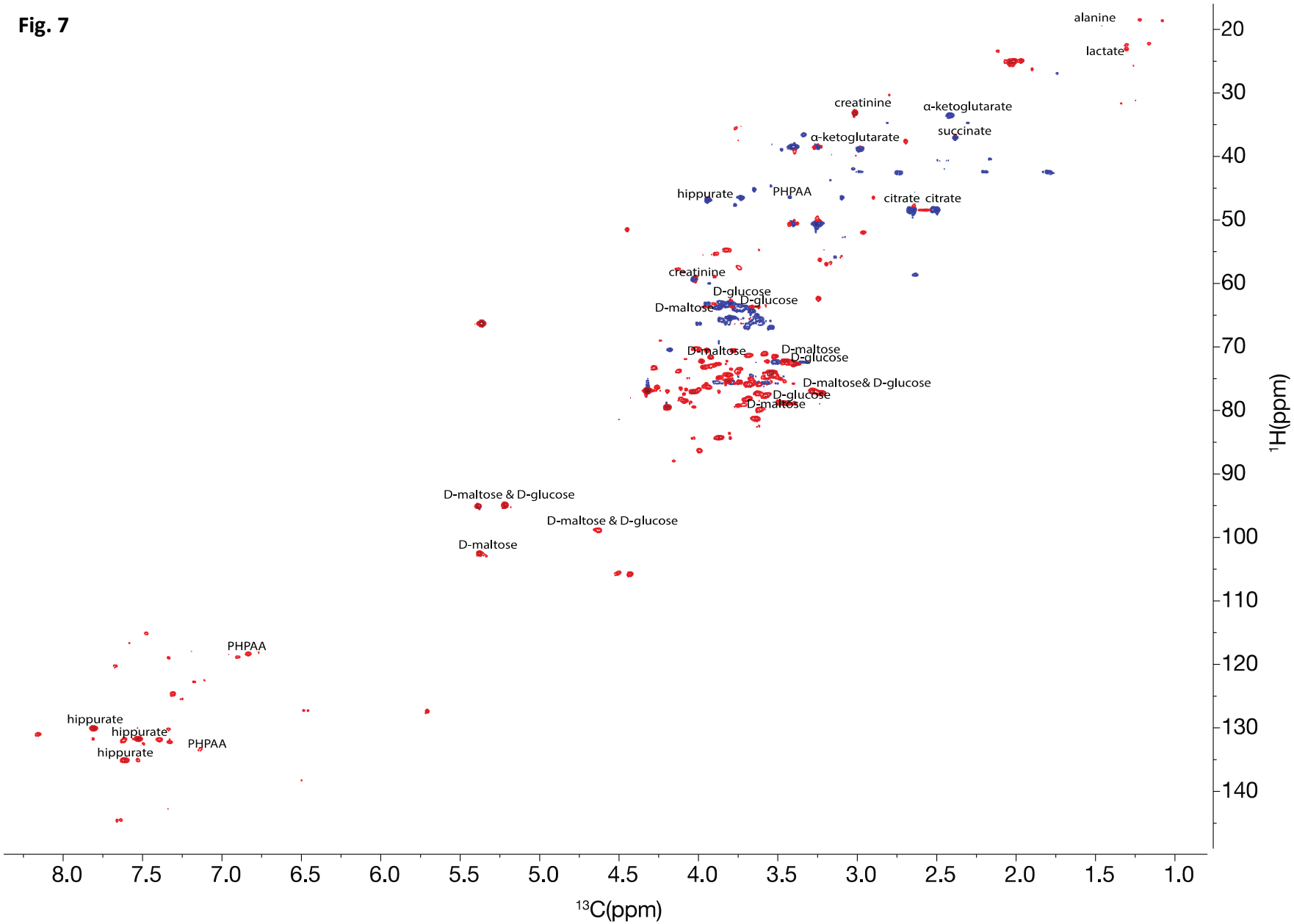
alanine
lactate
creatinine
α-ketoglutarate
succinate
α-ketoglutarate
hippurate
PHPAA
citrate
citrate
creatinine
D-glucose
D-glucose
D-maltose
D-maltose
D-maltose
D-glucose
D-maltose& D-glucose
D-glucose
D-maltose
D-maltose & D-glucose
D-maltose & D-glucose
D-maltose
PHPAA
hippurate
hippurate
PHPAA
hippurate
20
30
40
50
60
70
80
90
100
110
120
130
140
^{1}H(ppm)
8.0
7.5
7.0
6.5
6.0
5.5
5.0
4.5
4.0
3.5
3.0
2.5
2.0
1.5
1.0
^{13}C(ppm)